Potential Formation in a High-Speed Plasma Flow along Converging Magnetic Field Lines

N. Sato, Y. Watanabe, R. Hatakeyama, and T. Mieno[(a)]
Department of Electronic Engineering, Tohoku University, Sendai 980, Japan
(Received 24 June 1988)

The formation of a potential is experimentally investigated in a high-speed collisionless plasma flow injected into a region of converging magnetic field lines. When the plasma passes through this region, a large increase in potential occurs there, resulting in electron acceleration along the magnetic field. A drastic end-plate effect on the generated potential is observed when the plasma comes in contact with the end plate.

PACS numbers: 52.35.Sb, 52.55.Jd, 94.10.Sm, 94.30.Kq

The formation of electrostatic potential in magnetized plasmas is of crucial importance in conjunction with particle acceleration in space plasmas.[1] Much attention has been paid to electric double layers from this point of view.[2] As proposed by Alfvén and Fälthammar,[3] however, a so-called "field-aligned potential difference" is also generated by the different pitch-angle anisotropies of electrons and ions along an inhomogeneous magnetic field. This mechanism of potential formation might be important as well in fusion-oriented plasmas with highly anisotropic velocity distributions. A high burning voltage of the Penning discharge in a magnetic mirror field was explained on the basis of this mechanism.[4] In an experiment on a mirror-confined plasma produced by electron cyclotron resonance, the potential profiles observed were considered to be related to the above mechanism,[5] although the potential difference was smaller than T_e/e (T_e, electron temperature; $-e$, electron charge).

A recent extension of the theory of Alfvén and Fälthammar has been carried out by Serizawa and Sato[6] and Washimi and Katanuma[7] in order to investigate a field-aligned potential difference in a high-speed collisionless plasma flow along converging magnetic field lines. According to them, a potential difference $\gg T_e/e$ should be formed with a scale length equal to the magnetic field variation, because the ion velocity distribution is highly anisotropic in contrast to the almost isotropic electron velocity distribution. Here we demonstrate a clear evolution of potential formation in such a plasma flow injected into a region of converging magnetic field lines, including an end-plate effect that is observed when the plasma flow is terminated by the end plate.

A plasma flow is produced in a modified single-ended Q machine, as shown in Fig. 1. Just as in an ordinary single-ended Q machine, a potassium plasma is produced by surface ionization of potassium atoms at a 5.2-cm-diam hot tungsten plate (HP) at one end of the machine.[8] In front of HP, however, a nickel grid G_1 (0.15-mm-diam wire, 40 mesh/in.) coated with BaO (or LaB_6) is positioned 1.0 cm from HP and is electrically grounded together with the vacuum chamber. In order to accelerate the potassium ions, a positive potential ϕ_{HP} is applied to HP with respect to G_1. Then, most of the electrons emitted from HP are reflected by G_1. But, G_1 is heated by the radiation from HP, yielding an electron emission large enough to neutralize the space charge provided by the accelerated ions. Thus, we have a plasma of accelerated ions and almost thermal electrons. In front of G_1, another stainless-steel grid G_2 of the same mesh size is set 1.5 cm from HP. G_2 is used as a gate to inject a plasma flow. When G_2 is biased negatively, for example, at $\phi_g \lesssim -10$ V, with respect to the plasma potential ($\simeq$0–1.0 V), there is almost no plasma beyond G_2. With a jump of ϕ_g up to the plasma potential, we inject a plasma flow which is finally terminated by a 8.0-cm-diam stainless-steel end plate at a distance $z=270$ cm from G_2. The end-plate potential ϕ_T is kept smaller than ϕ_{HP} so that the accelerated ions are absorbed by the end plate. The plasma density n is around 1×10^8 cm^{-3} and $T_e\simeq0.15$ eV. The flow speed V_0 [$\simeq(2\psi_b/M)^{1/2}$, M is ion mass] is varied in the range $V_0/C_s=5$–26 [$C_s=(T_e/M)^{1/2}$] by changing ϕ_{HP} ($\simeq\psi_b/e$, 2–50 V). An ion energy spread $\Delta\psi_b\lesssim1$ eV is uniform in the directions parallel and perpendicular to the magnetic field. The background gas pressure is 1×10^{-6} Torr. Under our conditions, the collision mean free paths of electrons and ions are longer than the plasma length. The plasma flow is introduced into a region of converging magnetic field lines, which is located in the central part of the machine. The magnetic field B, 0.6 kG, is uniform between HP and the region of $\nabla B>0$. B is also uniform beyond the region of $\nabla B>0$ up to the end plate, where B

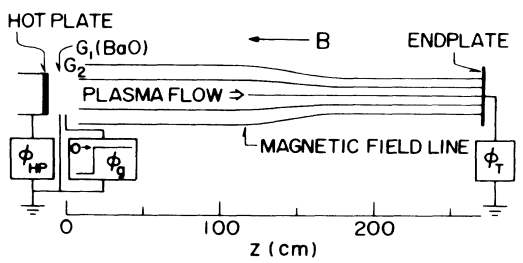

FIG. 1. Schematic of setup and magnetic configuration.

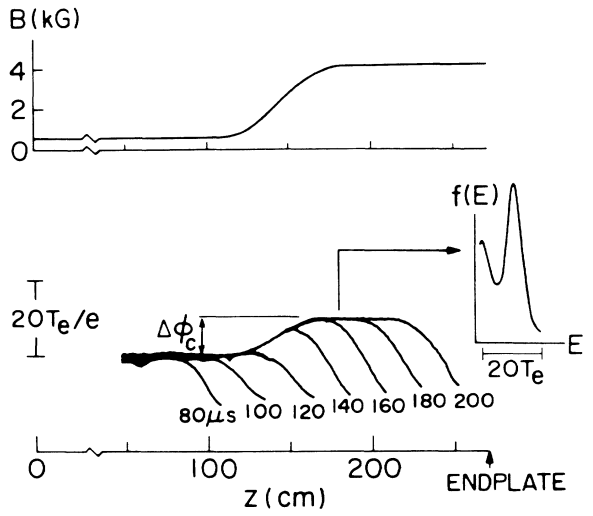

FIG. 2. Evolution of plasma potential in a plasma flow with $V_0/C_s=20$ (lower) passing through a region of $\nabla B>0$ with $R_m=7.0$ (upper), together with electron energy distribution $f(E)$ measured at $z=180$ cm and $t=180$ μs.

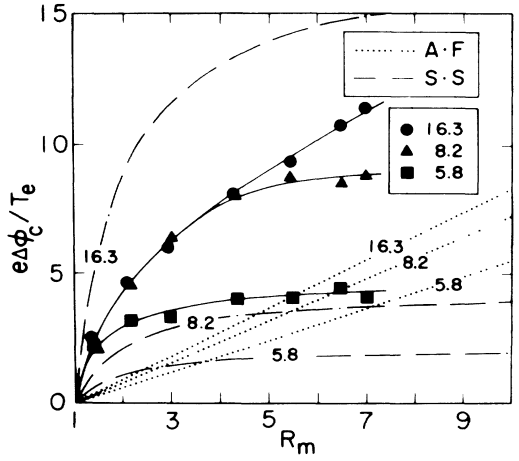

FIG. 3. Normalized potential difference $e\Delta\phi_c/T_e$ as a function of R_m with V_0/C_s ($=5.8$, 8.2, 16.3) as a parameter, before the plasma comes in contact with the end plate with $\phi_T=-20$ V, together with the theories of Alfvén and Fälthammar (AF) and of Serizawa and Sato (SS).

($=0.6$–4.5 kG) is changed so as to vary the mirror ratio R_m in the range of 1.0–7.5. Small movable Langmuir probes and grided analyzers are used to measure n, T_e, and V_0, and also the electron and ion energy distributions. The plasma potential ϕ is measured by a small emissive probe with high time resolution ($\simeq 1$ μs),[9] which is axially movable at the center of the plasma cross section.

A typical evolution of potential formation is shown for $V_0/C_s=20$ ($\phi_{HP}=30$ V) and $R_m=7.0$ in Fig. 2, where $\phi_T=-20$ V. Since V_0 is so large that the ion pitch-angle distribution is highly shifted in the direction toward the end plate, most of the ions pass through the region of $\nabla B>0$, being finally absorbed by the end plate. A fraction of the electrons are reflected by ∇B. The electrons that pass through toward the end plate are reflected by ϕ_T. The plasma, which is injected at t (time) $=0$, flows along the magnetic field, being accompanied by potential profiles as presented at subsequent times in Fig. 2. Before the plasma reaches the region of $\nabla B>0$ ($t\lesssim 80$ μs), ϕ is almost spatially constant up to the plasma front region, where ϕ decreases monotonically. In the plasma passing through the region of $\nabla B>0$, however, a spatial increase in ϕ is observed. After the plasma front passes through this region ($t\gtrsim 160$ μs), the potential increase $\Delta\phi_c$ generated there is about $10.7T_e/e$ and ϕ is again constant beyond the region of $\nabla B>0$ up to the plasma front region. These features and the $\Delta\phi_c$ measured do not depend on ϕ_T (<0). For $\phi_T>0$, the potential structure in the region of the plasma front up to the end plate is modified by a spatial increase of the vacuum potential toward the end plate. But, the ϕ profiles up to the plasma front region at various times and the $\Delta\phi_c$ in the region of $\nabla B>0$ are independent of ϕ_T, being the same as in case of $\phi_T<0$ unless the plasma comes in contact with the end plate.

The electron energy distribution function $f(E)$ parallel to the magnetic field is obtained from a derivative of the Langmuir-probe characteristics. The result is also presented in Fig. 2, where the measured position is on the side of higher magnetic field ($z=180$ cm) just beyond the region of $\nabla B>0$ at $t=180$ μs. There are two peaks in $f(E)$. The separation between them corresponds to the observed $e\Delta\phi_c$. This means that the peak with higher energy is due to electron acceleration by $\Delta\phi_c$, although most of the electrons accelerated are reflected by $\nabla\phi$ (<0) in the plasma front region. The other peak is observed at a probe potential around the plasma potential, indicating the existence of stationary electrons with finite energy spread.

In Fig. 3, $e\Delta\phi_c/T_e$ is plotted against R_m with V_0/C_s as a parameter. With an increase in R_m, $\Delta\phi_c$ increases initially, followed by a gradual saturation. The value of R_m at which this saturation starts increases as V_0 increases. At a fixed value of R_m, for example, at $R_m=7.0$, $\Delta\phi_c$ is observed to increase with an increase in V_0, but $e\Delta\phi_c/T_e\simeq 11$, independent of V_0, for $V_0/C_s\gtrsim 10$. This saturation appears at a smaller value of V_0 when R_m is smaller.

An effect of ϕ_T on the ϕ profiles is observed after the plasma front comes in contact with the end plate. In Fig. 4, the ϕ profiles for $\phi_T=15$ and -20 V are presented at $t=220$ and 300 μs, together with those in a final state ($t=\infty$) under the same conditions as in Fig. 2. The front tail of the plasma flow reaches the end plate at $t\simeq 220$ μs. For $\phi_T=15$ V, the plasma front is strongly modified by ϕ_T even at $t=220$ μs. After the plasma comes in contact with the end plate, there appears a drastic increase of the potential difference in the region

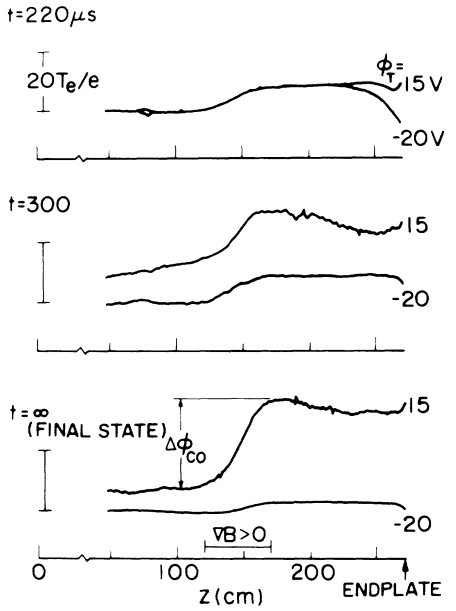

FIG. 4. Temporal evolutions of potential profiles after the plasma comes in contact with the end plate with $\phi_T = 15$ V and -20 V at $V_0/C_s = 20$ and $R_m = 7.0$.

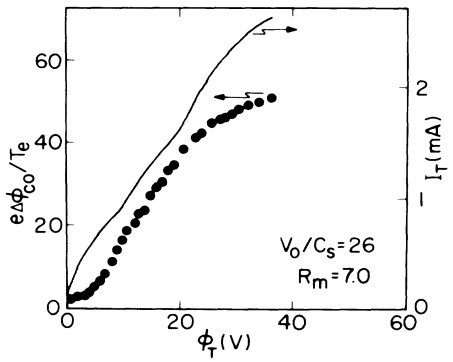

FIG. 5. Normalized potential difference $e\Delta\phi_{c0}/T_e$ and end-plate electric current I_T as a function of end-plate potential ϕ_T in a steady plasma flow with $V_0/C_s = 26$ and $R_m = 7.0$.

of $\nabla B > 0$, in addition to an increase of ϕ in the whole plasma region along the magnetic field. In the final state ($t \gtrsim 500$ μs), the potential difference is again localized in the region of $\nabla B > 0$, although ϕ decreases spatially beyond the region of $\nabla B > 0$ toward the end plate. The final difference $\Delta\phi_{c0}$ in the region of $\nabla B > 0$ is about $30T_e/e$ ($\simeq 2.8\Delta\phi_c$). On the other hand, for $\phi_T = -20$ V, there appears a gradual decrease of the potential difference in the region of $\nabla B > 0$ after the plasma reaches the end plate.

The dependence of $\Delta\phi_{c0}$ on ϕ_T is shown at $V_0/C_s = 26$ and $R_m = 7.0$ in Fig. 5. For $\phi_T < 0$, $e\Delta\phi_{c0}/T_e = 1.0$–$2.0$, independent of ϕ_T. For $\phi_T > 0$, however, $\Delta\phi_{c0}$ increases with an increase in ϕ_T. The electric current I_T passing through the end plate is also plotted against ϕ_T in Fig. 5. It is to be noted that $\Delta\phi_{c0}$ and I_T increase, roughly speaking, in a similar way with an increase in ϕ_T. These properties are also observed at different values of V_0/C_s and R_m.

As described above, the potential differences, $\Delta\phi_c$ and $\Delta\phi_{c0}$, which are obtained, respectively, before and after the plasma comes in contact with the end plate are larger than T_e/e, except $\Delta\phi_{c0}$ at $\phi_T < 0$. In our case, the average ion pitch angle θ is given by

$$\sin\theta \simeq \theta \simeq (\Delta\psi_b/\psi_b)^{1/2} \quad (\psi_b \gg \Delta\psi_b).$$

Therefore, when $R_m^{-1} \gg \sin^2\theta$, i.e., $\psi_b \gg R_m \Delta\psi_b$, and $\psi_b \gg e\Delta\phi_c$ (or $e\Delta\phi_{c0}$), the ions pass through the region of $\nabla B > 0$ without appreciable deceleration by ∇B and $\Delta\phi_c$ (or $\Delta\phi_{c0}$). Then, ion flux conservation yields $n_{i\mathrm{II}}/n_{i\mathrm{I}} \simeq R_m$, where $n_{i\mathrm{I}}$ and $n_{i\mathrm{II}}$ are the ion densities in the regions of $\nabla B = 0$ on the sides of lower and higher magnetic field, respectively. In the steady plasma flow at $\phi_T < 0$, we can assume the Boltzmann relation for electrons and charge neutrality on the both sides. Thus, the potential difference $\Delta\phi$ generated should satisfy $e\Delta\phi/T_e \simeq \ln R_m$. This relation predicts $e\Delta\phi/T_e \lesssim 2$ for $R_m \lesssim 7$, which is quite consistent with the $\Delta\phi_{c0}$ observed at $\phi_T < 0$, as in our previous experiment.[10]

According to Alfvén and Fälthammar,[3] the potential difference $\Delta\phi$ is given by $e\Delta\phi/T_e \simeq (1 - \Delta\psi_b/\psi_b)(R_m - 1)$ under our conditions. This relation predicts that $e\Delta\phi/T_e$ increases with a decrease in the ion pitch angle $\theta \simeq (\Delta\psi_b/\psi_b)^{1/2}$ ($\psi_b \gg \Delta\psi_b$) and/or with an increase in R_m, as expected physically. For $\psi_b/\Delta\psi_b \to \infty$, $\Delta\phi$ does not depend on ψ_b. These dependences are qualitatively similar to our observations. The above relation (AF) is plotted against R_m for three values of $\psi_b/\Delta\psi_b$ in Fig. 3, where $\Delta\psi_b = 1$ eV and $V_0/C_s = 5.8$, 8.2, and 16.3 correspond to $\psi_b = 2.5$, 5.0, and 20.0 eV, respectively. The measured results are found to have a much stronger dependence on V_0/C_s in comparison with the prediction. In addition, the observed saturation of $\Delta\phi_c$ with an increase in R_m is not predicted by the theory. On the other hand, Serizawa and Sato[6] obtained a semiempirical formula in their numerical analysis. It is written as

$$e\Delta\phi/T_e \simeq (\psi_b/\Delta\psi_b)(1 - 1/R_m)(1 + T_e/\Delta\psi_b)^{-1}$$

in our case, also predicting that $e\Delta\phi/T_e$ increases with a decrease in $(\Delta\psi_b/\psi_b)^{1/2}$ and/or with an increase in R_m. But, $e\Delta\phi/T_e$ is proportional to ψ_b, being accompanied by no saturation, and does not depend on R_m for $R_m \gg 1$, in contrast to the theory of Alfvén and Fälthammar. In Fig. 3, a difference is still found between this semiempirical relation (SS) and the experimental data. There are some qualitative agreements among the above two theories and our observations, but neither of the theories agrees quantitatively with our results. As pointed out in Ref. 7, particles trapped in a well of effective potential

$\Phi = \mu B - e\phi$ (μ, magnetic moment) might have to be taken into account precisely in actual situations.

The analyses mentioned above were performed on the plasma flow with no electric current. Thus, our end-plate potential and the resulting electric current were out of the scope of those works. In our experiment, however, a great change of ϕ appears after the plasma front reaches the end plate with $\phi_T > 0$. As in the double-layer experiment,[11] ϕ increases initially in the whole plasma region. It seems reasonable that this increase of ϕ is finally localized in the region of $\nabla B > 0$, reminding us of the potential jump in the constricted discharge tube.[12] We do not find a double-layer dynamics such as in Ref. 13, where $\phi_T > 0$ for the end plate to absorb electrons but to reflect ions in a uniform magnetic field. In our work, ions are absorbed by the end plate even if $\phi_T > 0$; this is also in contrast to an experiment[14] on double-layer formation due to ion reflection in a region of $\nabla B > 0$.

In summary, a large potential increase has been observed in a high-speed collisionless plasma flow passing through a region of converging magnetic field lines. This is the first laboratory demonstration of the field-aligned potential formation due to different pitch-angle anisotropies of electrons and ions in such a plasma flow, although we do not find a good agreement with the theories derived under simplified conditions. The effect of the end-plate potential is quite drastic, showing the importance of boundary-connected electric current in the potential formation.

We have enjoyed helpful conversations with T. Sato and H. Washimi. The work was supported by Grant-in-Aid for Scientific Research from the Ministry of Education, Science, and Culture, Japan.

[a]Permanent address: Department of Physics, Shizuoka University, Shizouka 422, Japan.

[1]C.-G. Fälthammar, Rev. Geophys. Space Phys. **15**, 457 (1977); *Physics of Auroral Arc Formation,* edited by S.-I. Akasofu and J. R. Kan (American Geophysical Union, Washington, DC, 1981); H. Alfvén, IEEE Trans. Plasma Sci. **14**, 616 (1986).

[2]H. Alfvén and P. Carlqvist, Solar Phys. **1**, 220 (1967); L. P. Block, Astrophys. Space Sci. **55**, 59 (1978); N. Sato, in *Proceedings of the Symposium on Plasma Double Layers, Roskilde, Denmark, 1982,* edited by P. Michelsen and J. Juul Rasmussen (Risø National Laboratory, Roskilde, 1982), p. 116; N. Hershkowitz, Space Sci. Rev. **41**, 351 (1985); H. Alfvén, IEEE Trans. Plasma Sci. **14**, 776 (1986).

[3]H.Alfvén and C.-G. Fälthammar, *Cosmical Electrodynamics* (Oxford Univ. Press, London, 1963), 2nd ed., p. 162. See also H. Persson, Phys. Fluids **6**, 1756 (1963), and **9**, 1090 (1966).

[4]N. Hopfgarten *et al.*, Phys. Fluids **11**, 2272 (1968).

[5]R. Geller *et al.*, J. Plasma Phys. **12**, 467 (1974).

[6]Y. Serizawa and T. Sato, Geophys. Res. Lett. **11**, 595 (1984), and Phys. Fluids **29**, 2753 (1986).

[7]H. Washimi and I. Katanuma, Geophys. Res. Lett. **13**, 897 (1986).

[8]R. W. Motley, *Q Machines* (Academic, New York, 1975); N. Sato *et al.*, Phys. Rev. Lett. **34**, 931 (1975).

[9]H. Fujita and S. Yagura, Jpn. J. Appl. Phys. **22**, 148 (1983).

[10]Y. Suzuki *et al.*, J. Phys. Soc. Jpn. **55**, 1568 (1986).

[11]N. Sato *et al.*, Phys. Rev. Lett. **46**, 1330 (1981).

[12]M. J. Schönhuber, Z. Angew. Phys. **15**, 454 (1963).

[13]S. Iizuka *et al.*, Phys. Rev. Lett. **48**, 145 (1982).

[14]R. L. Stenzel *et al.*, Phys. Rev. Lett. **45**, 1497 (1980).